Using Optical Flow Fields for Polyp Detection In Virtual Colonoscopy

Burak Acar[1], Sandy Napel[1], David Paik[1], Burak Göktürk[2], Carlo Tomasi[3], and Christopher F. Beaulieu[1]

[1] Stanford University, Department of Radiology
LUCAS MRS Center, 3D Lab., Stanford, CA 94305-5488, USA
bacar, snapel @stanford.edu
paik@smi.stanford.edu, cfb@s-word.stanford.edu
URL: www.3dradiology.org
[2] Stanford University, Electrical Engineering Department
Stanford, CA 94305, USA
[3] Stanford University, Computer Science Department
Stanford, CA 94305, USA

Abstract. Since the introduction of Computed Tomographic Colonography (CTC), research has mainly focused on visualization and navigation techniques. Recently, efforts have shifted towards computer aided detection (CAD) of polyps. We propose a new approach to CAD in CT images that attempts to model the way a radiologist recognizes a polyp using optical flow fields (OFF). Features extracted from OFFs are used by a linear classifier for polyp detection. An initial validation of our technique resulted in an average of 75% specificity at 100% sensitivity in a 10-fold cross validation study on a set of 220 polyp-like structures, 20 of which were true polyps.

1 Introduction

Computed Tomographic Colonography (CTC) was suggested in the early 1980's and realized in the 1990's as a minimally invasive method that would make mass screening of colorectal cancer feasible [1–4]. Since then several studies were conducted to assess the performance of CTC [5–10]. In almost all studies, CTC was based on the examination of CT images by an expert radiologist, using either the 2D images, 3D virtual colonoscopic views or both. Thus, until recently most efforts were directed towards developing better visualization and navigation techniques [4, 11–19]. Lately, more effort has been put into computer aided detection (CAD), whose ultimate goal is to identify polyps in a 3D CT data efficiently, and with high sensitivity and specificity. Mir et al. reviews a set of techniques that can be used for shape description in CT images [20]. We are aware of two studies on CAD in CTC: Summers et al. reported a shape based polyp detector and concluded that CAD is feasible in CTC [21] and Paik et al. proposed a Hough Transform-based polyp detector [22, 23]. However, these CADs suffer from low specificity, which would require radiologists to examine a large number of CAD hits to rule out false detections.

The goal of our research is to develop a highly sensitive and specific CAD for CTC. We attempted to model the way a radiologist recognizes a polyp by focusing on the changes in consecutive images as one views sequential cross-sections of the volumetric source CT data (3D CT data). We used Optical Flow Fields (OFF) to represent these changes, and a linear classifier acting on these features to recognize true polyps.

2 Method

2.1 Data Acquisition

Patients were imaged in the supine position after colon cleansing and air-insufflation of the colon on a GE HiSpeed Advantage single detector or GE LightSpeed multi-row detector scanner (GE Medical Systems, Milwaukee, WI). Typical acquisition parameters were 3 mm collimation, pitch 1.5-2.0, 1.5 mm reconstruction interval, 120 KVp, 200 MAs for the single detector scanner and 2.5 mm collimation, pitch 3.0, 1.0-1.5 mm reconstruction interval, 120 KVp, 56 MAs for the multi-row detector scanner. Data were stored as 2 byte unsigned integers. The size of the 3D data matrix was $512 \times 512 \times N$, N is the number of axial slices. N is typically around 350. The average voxel spacing was $0.74mm \times 0.74mm \times 1.31mm$.

2.2 Initial Detection

The data was preprocessed by a Hough Transform-based polyp detector (HTD) [22, 23]. HTD basically computes the normals to an isointensity surface and searches for voxels at which a large number of normals intersect. Defining the number of normals that intersect in a given voxel as the HT score of that voxel, a threshold is applied for detection. Typically the voxels at the centers of spherical structures have high scores. The detected voxels mark the locations of polyps with high sensitivity but low specificity. We extracted a subvolume consisting of $21 \times 21 \times 21$ voxels centered on each detection with a score above a fixed threshold.

2.3 Optical Flow Field Computation

The aim of the OFF computation is to characterize the change in the location of the edges (tissue/air boundary) in the image plane while scrolling back and forth along the third dimension. This third dimension can be thought as the time axis [24]. If we name the image plane as the xy-plane then the basic optical flow equation is [25]:

$$\nabla I.\mathbf{v} + \frac{\partial I}{\partial t} = 0 \tag{1}$$

where $\mathbf{v}(x, y)$ is the OFF and $I(x, y)$ is the image, i.e. the intensity function. Equation 1 allows only the computation of $\mathbf{v}_\perp$, the component along the local

∇I. This serves to our purpose and it is simple. We will refer to $\mathbf{v}_\perp$ as $\mathbf{v}$ in what follows.

Keeping in mind that the coordinates of the voxel detected by HTD (HT_hit) is $(0,0,0)$, $\mathbf{v}_t(x,y)$ is computed for $x,y,t \in [-10,10]$. t is first incremented from 0 to 10 and then from 0 to -10. This is equivalent to moving outwards from the center. This assures the consistency in the direction of motion of the edges of spherical structures. $\mathbf{v}_t(x,y)$ are summed and the resulting OFF is filtered with a moving average filter of window size of 3×3 $cells$ as

$$\mathbf{v}_i(x,y) = Moving\_Average\left(\Sigma_t \mathbf{v}_t(x,y)\right) \ , i \in X,Y,Z \tag{2}$$

Each $\mathbf{v}_i(x,y)$ corresponds to scrolling along the direction i.

2.4 Optical Flow Field Characterization

The OFF characterization starts with the detection of the parent and the child nodes. The parent node is defined to be the minimum divergence point in the vicinity (± 2 $cells$) of the HT_hit. This is the most likely location of the center of a polyp. The child nodes are defined to be the points on the incoming streamlines, 5 units away from the parent node. There are 8 child nodes, each corresponding to a streamline ending at a different immediate neighbor of the HT_hit.

A topology based quantitative characterization of the $\mathbf{v}_i(x,y)$, $i \in X,Y,Z$, at the parent node, is employed. It is represented as a point on the 2D $\alpha\beta$-plane, where α and β are defined as follows [26]. Let

$$\mathbf{J} = \begin{bmatrix} \frac{\partial v_x}{\partial x} & \frac{\partial v_x}{\partial y} \\ \frac{\partial v_y}{\partial x} & \frac{\partial v_y}{\partial y} \end{bmatrix}, \tag{3}$$

$$P = -trace(\mathbf{J}), \tag{4}$$

$$Q = |\mathbf{J}|, \tag{5}$$

then

$$\alpha = -P, \tag{6}$$

$$\beta = sign(P^2 - 4Q)\sqrt{|P^2 - 4Q|}. \tag{7}$$

α and β essentially carry the information present in the eigenvalues of the characteristic equation

$$\lambda^2 + P\lambda + Q = 0 \tag{8}$$

They depend on the local divergence, curl and magnitude of the OFF. The origin of the $\alpha\beta$-plane corresponds to a uniform OFF.

As the third feature, the angular spread of the locations of child nodes around the parent node is defined as

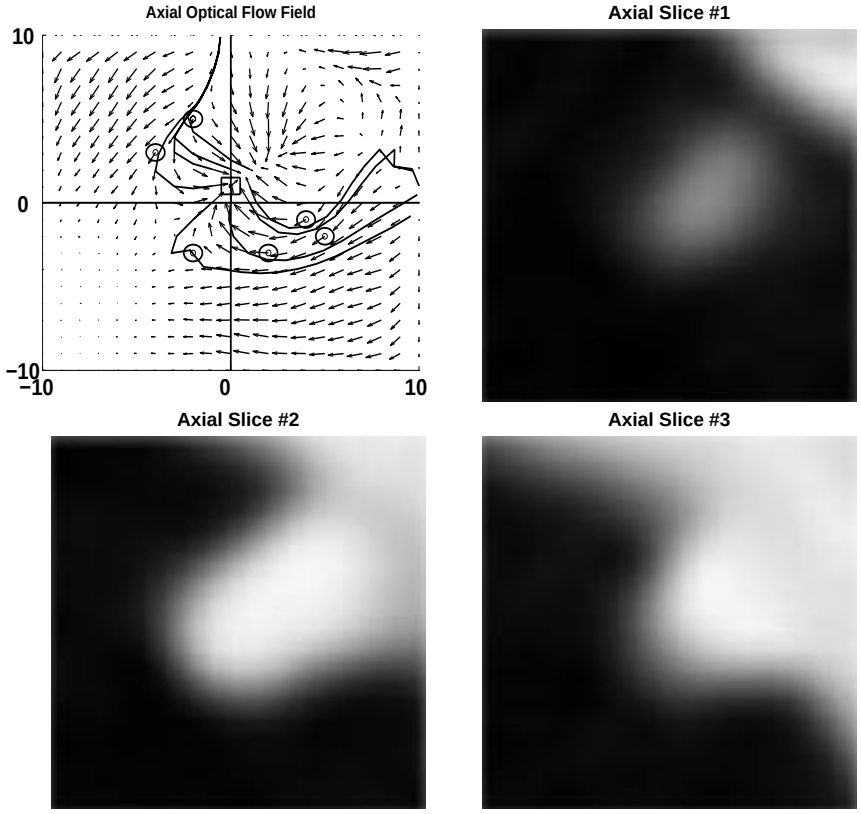

Fig. 1. 3 axial images (smoothed for visual purposes) and the axial OFF. The parent node is marked with a small square and the child nodes are marked with small circles. 3 of the 8 child nodes are coincident.

$$d = \frac{1}{8}\Sigma_i \left(\sqrt{\Sigma_j \theta_{ij}^2}\right) \ , \ \theta_{ij} = \angle(child_i, child_j) \in [0, \pi], \tag{9}$$

taking the parent node as the origin. Larger d's indicate increased spread of the child nodes around the parent node.

The 3D feature vector, $[\alpha \ \beta \ d]$, is computed for all three $\mathbf{v}_i(x, y)$, $i \in X, Y, Z$. The median value for each feature is used in the final 3D feature vector used for classification. Figure 1 shows three axial images of a polyp, corresponding to three different t values (the image plane is the axial plane) and the computed OFF associated with this t-axis ($t \equiv z$).

3 Preliminary Analysis

Data were acquired from 8 patients (7 male and 1 female with age 41-85, mean age 63) as described in Section 2.1. Preprocessing with a HT score threshold

of 10000 resulted in 220 HT_hits. Fiber optic colonoscopy results showed that 7 patients had a total of 20 polyps and that all polyps were detected by HTD. This means that the HTD, with the current threshold value, had 100% sensitivity and a high false positive rate. These 220 HT_hits were used as inputs to our algorithm.

We randomly divided the data set into 10 equal size mutually exclusive subsets, such that each subset contains 2 true positive and 20 false positive HT_hits. For each of 10 experiments, one of these subsets was used as the test set and the remaining nine subsets were used for training. We used a Mahalanobis distance based classifier. The Mahalanobis distance of a vector $\mathbf{f}$ to the mean vector, $\mathbf{m}_\Gamma$, of a population, Γ, is defined as [27],

$$r_{\mathbf{f},\mathbf{m}_\Gamma} = \sqrt{(\mathbf{f}-\mathbf{m}_\Gamma)^T \mathbf{C}_\Gamma^{-1} (\mathbf{f}-\mathbf{m}_\Gamma)} \tag{10}$$

where $\mathbf{C}_\Gamma$ is the covariance matrix of Γ. We added a bias term, b, to r that is used to trade off specificity and sensitivity of the classifier as

$$\begin{aligned} r_{\mathbf{f},\mathbf{m}_{\Gamma_1}} - r_{\mathbf{f},\mathbf{m}_{\Gamma_0}} + b \leq 0 \Rightarrow \mathbf{f} \in \Omega_1 \\ \text{otherwise} \Rightarrow \mathbf{f} \in \Omega_0 \end{aligned} \tag{11}$$

where, Γ represents the training set and $\mathbf{f}$ represents a sample from the test set, Ω. The subscript '1' refers to the subset of true positives, while the subscript '0' refers to the subset of true negatives.

In an attempt to assess the potential of OFFs in polyp identification, we measured the maximum specificity at 100% sensitivity, for each experiment, where the specificity was defined as the percentage of correctly identified non-polyp structures in each test set. The maximum specificity values at 100% sensitivity for each experiment was: 0.85, 0.85, 0.35, 0.90, 1.00, 0.15, 0.80, 0.80, 0.85, 0.95.

The analysis of an individual subvolume lasted 3.0 seconds using Matlab^{TM} 6.0 (The Mathworks Inc., MA, USA) on a PC with 1GHz Pentium III processor. The time measurements exclude the subvolume extractions.

4 Discussion

Our ultimate goal is to decrease the radiologists' reading time by directing them towards the true polyps. To do this, we model the way a radiologist recognizes a polyp in 3D CT data based on the motion of edges as one scrolls back and forth through parallel planes transecting a suspicious structure. It is obvious that the choice of scrolling direction affects the computed OFF. We tried to decrease this dependency by performing the analysis in three orthogonal directions and using the median values of each feature. A more robust approach would be to use multiple scrolling directions and construct a feature vector out of the histograms of measured feature values. Using additional features, like the homogeneity of the region of interest, might also improve performance.

We have observed that the divergence of the OFF at the parent node is of particular relevance for polyp identification. As such, the α and β parameters

derived from the Jacobian of the OFF are very appropriate because they not only represent the information in the eigenvalues of the Jacobian matrix, but also the parameter α directly corresponds to the divergence of the OFF.

One of the two polyps in the test set of experiment 3 was completely hidden on the sagittal plane and could be seen properly only in the coronal plane. The median operation eliminated the measurements from the coronal plane, degrading the performance of the system (specificity was 0.35). The low specificity level of experiment 6 (0.15), on the other hand, is due to the large cancerous tumor (3.2cm in diameter) in the test set. Such big structures cannot be detected by OFFC with the current parameters, especially the subvolume size. These observations also suggest that increasing the number of scrolling directions would improve the performance.

The classifier we used performs linear discriminant analysis based on the minimization of the Mahalanobis distance between the learning and the test samples. The advantages of using the Mahalanobis distance are: *(i)* It automatically accounts for scaling, *(ii)* it takes care of the correlation between features and *(iii)* it can provide linear and curved decision boundaries. Another possible classifier would be the Support Vector Machines (SVM) [28]. SVMs are capable of trading off the training error with the generalization error. They can work practically in infinite dimensional feature spaces. The choice of the parameters and the feature space is critical for SVMs' performance and is the subject of future work. SVMs can even be used to learn directly from the computed OFFs, without extracting specific parameters, like α, β, d. This requires an appropriate kernel definition.

Our method is aimed to improve the HT-based CAD results by increasing the specificity without sacrificing sensitivity at a given operating point set by the HTD threshold. The specificity levels given in Section 3 show the achievable specificity levels at the operating point corresponding to the HTD threshold of 10000. It should be noted that in this data set HTD performs with high specificity levels (average of maximum specificity level over 10 experiments is $84 \pm 20\%$ at 100% sensitivity) at some other operating points. The improvement due to OFFC in specificity at those operating points would be different. Thus a direct comparison of this mean specificity level with that of OFFC post-processed data (mean specificity of $75 \pm 27.5\%$ at 100% sensitivity) is not possible. Moreover, the correlation coefficient between HT scores and the α, β, d parameters are -0.44, -0.05, 0.14, respectively. These results also support that the OFFC parameters assess different qualities of the CTC data. A more detailed analysis is given in [29, 30].

The results presented here demonstrate the relevant information in OFFs for polyp detection in virtual colonography. However, higher specificity levels are required for practical clinical applications. Typically, the HTD threshold needs to be set low enough for 100% sensitivity, and that results in high false positive rates. Recent experiments that we conducted on a larger dataset that has low specificity at 100% sensitivity using HTD alone showed a significant increase in specificity without sacrificing the sensitivity set by HTD parameters [29, 30].

It would also be possible to use the present method to detect polyps directly from the 3D CT data without the need for the HTD. The OFFs associated with different scrolling directions could be computed for the whole volume and then classification could be performed only in the vicinity of the colon, based on α, β and d values.

5 Conclusion

We showed that the idea of modeling the way a radiologist recognizes polyps in 3D CT data is feasible. Optical flow fields (OFF) provide a robust framework for quantitative analysis of inter-slice relations in the 2D CT images. Although many different features can be extracted from OFFs, we showed that α, β and d carry relevant information for polyp recognition. However, several other features may be useful to obtain better performance. Further research is required to optimize the feature space and the classifier.

References

1. Coin, C.G., Wollett, F.C., et al.: Computerized radiology of the colon: a potential screening technique. Comput. Radiol. **7(4)** (1983) 215–221
2. Chaoui, A.S., Blake, M.A., et al.: Virtual colonoscopy and colorectal cancer screening. Abdom. Imaging **25(2)** (2000) 361–367
3. Johnson, C.D., Dachman, A.H.: CT colonography: the next colon screening examination? Radiology **216(2)** (2000) 331–341
4. Vining, D.J.: Virtual colonoscopy. Gastrointest. Endosc. Clin. N. Am. **7(2)** (1997) 285–291
5. Hara, A.K., Johnson, C.D., et al.: Detection of colorectal polyps by computed tomographic colography: feasibility of a novel technique. Gastroenterology **110(1)** (1996) 284–290
6. Macari, M., Milano, A., et al.: Comparison of time-efficient CT colonography with two- and three-dimensional colonic evaluation for detecting colorectal polyps. Am. J. Roentgenol **174(6)** (2000) 1543–1549
7. Hara, A.K., Johnson, C.D., et al.: Detection of colorectal polyps with CT colography: initial assessment of sensitivity and specificity. Radiology **205(1)** (1997) 59–65
8. Rex, D.K., Vining, D., et al.: An initial experience with screening for colon polyps using spiral CT with and without CT colography. Gastrointest. Endosc. **50(3)** (1999) 309–313
9. ASGE, American Society for Gastrointestinal Endoscopy: Technology status evaluation: virtual colonoscopy: November 1997. Gastrointest. Endosc. **48(6)** (1998) 708–710
10. Dachman, A.H., Kuniyoshi, J.K., et al.: CT colonography with three-dimensional problem solving for detection of colonic polyps. Am. J. Roentgenol **171(4)** (1998) 989–995
11. Paik, D.S., Beaulieu, C.F., et al.: Visualization modes for CT colonography using cylindrical and planar map projections. J. Comput. Assist. Tomogr. **24(2)** (2000) 179–188

12. Kay, C.L., Kulling, D., et al.: Virtual endoscopy – comparison with colonoscopy in the detection of space-occupying lesions of the colon. Endoscopy **32(3)** (2000) 226–232
13. Lee, T.Y., Lin, P.H., et al.: Interactive 3D virtual colonoscopy system. IEEE Trans. Inf. Tech. Biomed. **3(2)** (1999) 139–150
14. Beaulieu, C.F., Jeffrey, Jr., R.B., et al.: Display modes for CT colonography. Part II. Blinded comparison of axial CT and virtual endoscopic and panoramic endoscopic volume-rendered studies. Radiology **212(1)** (1999) 203–212
15. Wang, G., McFarland, E.G., et al.: GI tract unraveling with curved cross sections. IEEE Trans. Med. Imaging **17(2)** (1998) 318–322
16. McFarland, E.G., Brink, J.A., et al. : Visualization of colorectal polyps with spiral CT colography: evaluation of processing parameters with perspective volume rendering. Radiology **205(3)** (1997) 701–707
17. Haker, S., Angenent, S., et al.: Nondistorting flattening maps and the 3D visualization of colon CT images. IEEE Trans. Med. Imaging **19** (2000) 665–670
18. Paik, D.S., Beaulieu, C.F., et al.: Automated flight path planning for virtual endoscopy. Med. Phys. **25(5)** (1998) 629–637
19. Samara, Y., Fiebich, M., et al.: Automated calculation of the centerline of the human colon on CT images. Acad Radiol. **6(6)** (1999) 352–359.
20. Mir, A.H., Hanmandlu, M., et al.: Description of shapes in CT images. IEEE EMBS Mag. **18(1)** (1999) 79–84
21. Summers, R.M., Beaulieu, C.F., et al.: Automated polyp detector for CT colonography: feasibility study. Radiology **216(1)** (2000) 284–290
22. Paik, D.S., Beaulieu, C.F., et al.: Computer aided detection of polyps in CT colonography: free response ROC evaluation of performance. Radiological Society of North America 86th Scientific Sessions, Chicago, IL, November, 2000.
23. Paik, D.S., Beaulieu, C.F., et al.: Detection of polyps in CT colonography: a comparison of a computer aided detection algorithm to 3D visualization methods. In: Proc. Radiological Society of North America 85th Scientific Sessions, Chicago, IL, November, 1999.
24. Yiu-Fai, W., Tsuhan, C.: Compression of medical volumetric data in a video-codec framework. ICASSP **4** (1996) 2128–2135
25. Beauchemin, S.S., Barron, J.L.: The computation of optical flow. ACM Computing Surveys **27(3)** (1995) 433–467
26. Lavin, Y., Batra, R., Hesselink, L.: Feature comparisons of vector fields using earth mover's distance. In: Proc. IEEE/ACM Visualization'98, North Carolina, October, 1998
27. Mahalanobis, P. C.: On the generalized distance in statistics Proc. Natl. Institute of Science of India, **12** (1936) 49-55
28. Vapnik, V.N.: The nature of statistical learning theory. New York : Springer, 1995
29. Acar, B., Beaulieu, C.F., et al.: Assessment of an optical flow field-based polyp detector for CT colonography. Submitted to the 23rd Annual Meeting of IEEE Engineering in Medicine and Biology Society, İstanbul, Turkey, 2001
30. Acar, B., Beaulieu, C.F., et al.: Optical flow field based-classification for improved detection of polyps in CT colonography. Submitted to IEEE Transaction on Medical Imaging